European Journal of Medicinal Chemistry 127 (2017) 275–285

Contents lists available at ScienceDirect

European Journal of Medicinal Chemistry

journal homepage: http://www.elsevier.com/locate/ejmech

Research paper

Discovery of novel anti-angiogenesis agents. Part 6: Multi-targeted RTK inhibitors

Lin Zhang [a, 1], Yuanyuan Shan [b, 1], Chuansheng Li [a], Ying Sun [a], Ping Su [a], Jinfeng Wang [a], Lisha Li [a], Xiaoyan Pan [a], Jie Zhang [a, *]

[a] School of Pharmacy, Health Science Center, Xi'an Jiaotong University, No. 76, Yanta West Road, Xi'an, Shaanxi Province, 710061, PR China
[b] Department of Pharmacy, The First Affiliated Hospital of Xi'an Jiaotong University, Xi'an, Shaanxi Province, 710061, PR China

ARTICLE INFO

Article history:
Received 26 October 2016
Received in revised form
29 December 2016
Accepted 30 December 2016
Available online 2 January 2017

Keywords:
Anti-angiogenesis agents
Multi-targeted
RTK inhibitors
Diaryl malonamide
Diaryl thiourea

ABSTRACT

Angiogenesis is modulated by a multitude of pro-angiogenic factors including VEGFR-2, Tie-2, and EphB4. Moreover, their crosstalk also had been well elaborated. We have identified several diarylurea-based VEGFR-2 inhibitors as potential anti-angiogenesis agents. As a continuation to our previous research, two series of diaryl malonamide and diaryl thiourea derivatives have been developed as multiplex VEGFR-2/Tie-2/EphB4 inhibitors. Interestingly, the biological evaluation indicated that several compounds bearing trifluoromethyl or trifluoromethoxyl exhibited promising multiplex inhibition against angiogenesis-related VEGFR-2, Tie-2, and EphB4. The representative compound (**18a**) displayed both potent multi-targeted RTK inhibition and considerable antiproliferative activities against human umbilical vein endothelial cells (EA.hy926). These results will contribute to the discovery of novel muti-targeted anti-angiogenesis agents.

1. Introduction

Angiogenesis plays an essential role in a number of physiological and pathological processes, including embryonic development, wound healing, tumor growth, and certain ocular diseases. Under normal physiological conditions, angiogenesis is strictly modulated by a multitude of pro-angiogenic and anti-angiogenic factors [1]. In tumor growth, to acquire and sustain microvascular network, cancer cells secrete many growth factors which could induce angiogenesis and promote tumor progression. Inhibition of angiogenesis is a promising and clinically validated approach for treatment of cancer. Angiogenesis is primarily mediated by growth factors that cause signal transduction, for the most part, via receptor tyrosine kinases (RTKs). Several angiogenic ligands and their corresponding RTKs play critical roles in angiogenesis. Moreover, the crosstalk between various RTKs had also been well elaborated [2]. Three subfamilies out of at least 14 RTK subfamilies, VEGF/VEGFR-2, Ang/Tie-2, and Ephrin B2/EphB4 are highly expressed in the endothelial cells (ECs) from embryonic to adulthood. Extensive studies have indicated that these three RTKs play an essential role in both vasculogenesis and angiogenesis [3]. VEGF is one of the most potent angiogenic growth factors, and its binding to VEGFR-2 induces signal transduction that promotes ECs survival, proliferation, and migration. Angiogenic growth factors (Ang) and their tyrosine kinase receptor (Tie-2) have been implicated in vessel stabilization, maturation, and remodeling of vasculature [4]. Recent reports indicated that Ephrin receptor tyrosine kinase (EphB4) and its transmembrane-type Ephrin B2 ligand are crucial for vascular development [5]. Therefore, these three RTKs, VEGFR-2, Tie-2, and EphB4, are considered to be promising targets for design and discovery of novel anti-angiogenesis agents.

In our previous research, we have focused on the discovery of novel VEGFR-2 inhibitors as anti-angiogenesis agents. Numbers of biphenyl-aryl ureas incorporated with salicylaldoxime have been developed as potent and selective VEGFR-2 inhibitor through structural optimization of Taspine (Fig. 1) [6–9]. Several nanomolar VEGFR-2 inhibitors with potential anti-angiogenesis activities have been identified [10–12]. These biphenyl-aryl ureas exhibited significantly VEGFR-2 inhibitory activity as well as anticancer potency. Among them, **BPS-7** was found to possess a reasonable anti-angiogenic potency. Further evaluation indicated that **BPS-7** could inhibit phosphorylation of VEGFR-2 and the formation of blood vessels. Moreover, it also significantly inhibited the proliferation

* Corresponding author.
E-mail address: zhj8623@xjtu.edu.cn (J. Zhang).
[1] Both authors contributed equally to this work.

http://dx.doi.org/10.1016/j.ejmech.2016.12.059
0223-5234/

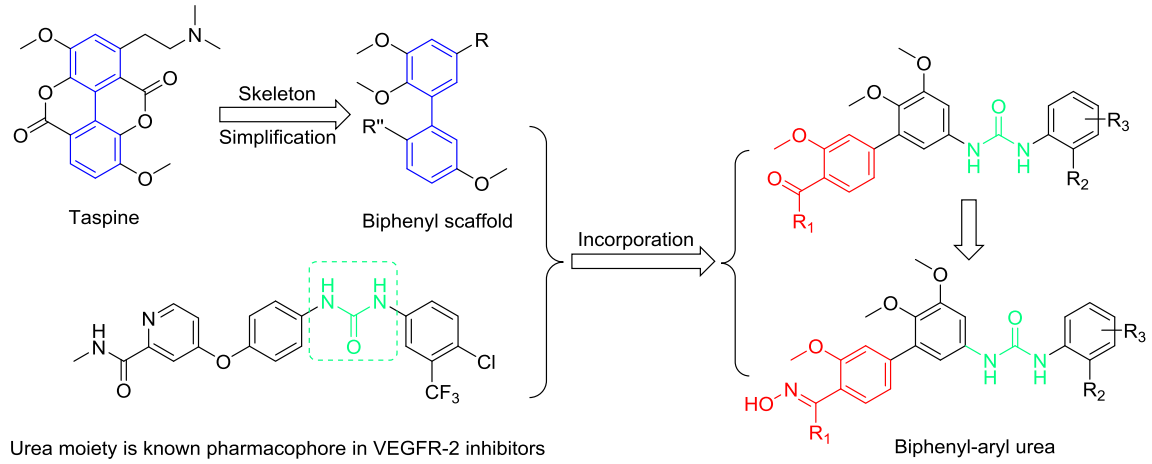

Fig. 1. Previous research on the discovery of biphenyl-aryl urea as novel VEGFR-2 inhibitors.

and migration of human umbilical vein endothelial cells [13]. Therefore, diaryl urea (**BPS-7**) could be considered as a promising lead compound for further optimized as novel anti-angiogenesis agents.

Angiogenesis is a complex process which are highly related with VEGFR-2, Tie-2, and EphB4. These three RTKs could stimulate endothelial proliferation in angiogenesis. Each of these RTKs has been considered as valid target of anti-angiogenesis agents [14]. This realization and the drug resistance of single target drugs have led researchers to speculate compounds which simultaneously inhibit multiple RTKs (multi-targeted inhibitors) might be a promising strategy. Encouraged by previous results, our further efforts focused on the discovery of novel anti-angiogenesis agents with multiplex inhibition profile. First of all, the urea moiety in lead compound was replaced with malonamide bearing more hydrogen-bond donors and acceptors. The two methoxyl groups on biphenyl have been removed in order to reduce the steric hindrance of inhibitors when binding with receptors. Meanwhile, replacements of salicylaldoxime by 1*H*-indazol-3-amine and quinazolin-2-amine were carried out to enhance the affinity of inhibitors with hinge region of RTKs. These heterocyclic amines bearing more hydrogen bond acceptors could retain the essential hydrogen bonds with hinge region. Moreover, various diverse substituents such as halogen, trifluoromethyl, trifluoromethoxyl and methylenedioxy were incorporated to terminal aniline. The design strategy and structures of the title compounds were represented in Fig. 2.

In our continuous efforts on the discovery of novel anti-angiogenesis agents, we designed and synthesized fourteen diaryl malonamides and ten diaryl thioureas as multi-targeted VEGFR-2/Tie-2/EphB4 inhibitors *via* structural optimization of previously reported VEGFR-2 inhibitors. Biological evaluations including enzymatic inhibition and antiproliferative potency were performed to yield novel anti-angiogenesis agents with multiplex inhibition profile. Molecular modeling studies were also carried out to rationalize the efficiency of the potent inhibitors. These derivatives exhibited potent anti-angiogenesis activity and could be considered as promising lead compounds for further development of novel anti-angiogenesis agents.

2. Results and discussion

2.1. Synthesis of title compounds

Two series of diaryl malonamide and diaryl thiourea derivatives have been yielded by using Pd-catalyzed Suzuki coupling reaction as key step. The preparation of title compounds (**10a~10n**) started with the synthesis of aminoindazole (**2**) from commercially available 2-fluoro-6-iodo-benzonitrile (**1**) by using five equiv of hydrazine monohydrate in refluxing ethanol under the presence of $NaHCO_3$ [15]. Subsequently, aminoindazole (**2**) and 4-aminophenylboronic acid (**3**) or 3-aminophenylboronic acid (**4**) were coupled by classical Pd-catalyzed Suzuki coupling reaction affording intermediates (**5**) and (**6**). Condensation of various aniline (**8a~8j**) with 1,1-cyclopropanedicarboxylic acid afforded (**9a~9j**). Finally, treatment of (**5**) or (**6**) with various intermediates (**9a~9j**) in the presence of triethylamine and 1-[Bis(dimethylamino)methylene]-1H-1,2,3-triazolo [4,5-b]pyridinium 3-oxide hexafluorophosphate (HATU) afforded the title compounds (**10a~10n**) [16] (see Scheme 1).

Diaryl thiourea (**18a~18j**) were readily prepared using the following synthetic route (Scheme 2). Commercially available aldehyde (**11**) was converted to 6-bromoaminoquinazoline (**12**) by treatment with guanidine carbonate heating in *N,N*-dimethylacetamide (DMA). Intermediate (**12**) was subsequently converted to (**14**) through Suzuki coupling with 4-aminophenylboronic acid (**13**) [17]. Various anilines were treated with CS_2 to yield (**16a~16j**), and then reacted with triphosgene (BTC) to produce various isothiocyanates (**17a~17j**) [18]. Finally, these isothiocyanates were treated with intermediate (**14**) in DCM to afford the second series of title compounds (**18a~18j**).

All of the title compounds were characterized by ^{1}H-NMR, ^{13}C-NMR, mass spectroscopy and melting point. ^{1}H-NMR, ^{13}C-NMR, mass spectroscopy, and melting point of all the title compounds are described in Supplementary Material.

2.2. RTK inhibitory activity

Enzymatic inhibition evaluation of title compounds against VEGFR-2, Tie-2, and EphB4 were performed using ADP-Glo Kinase Assay Kit (Promega, Wisconsin, USA). The biological evaluation results were depicted in Table 1 and Table 2 with Sorafenib as positive control. The majority of the title compounds exhibited moderate to good inhibitory potency. As shown in Table 1, replacement of urea with malonamide yielded several potent multi-targeted compounds with multiplex inhibition profile. Four compounds (**10a, 10b, 10g**, and **10i**) of them exhibited promising activity with nanomolar IC_{50} values less than 50 nM. Compound (**10g**) displayed comparable RTK inhibitory potency to Sorafenib with IC_{50} values less than 25 nM. It also showed the most potent

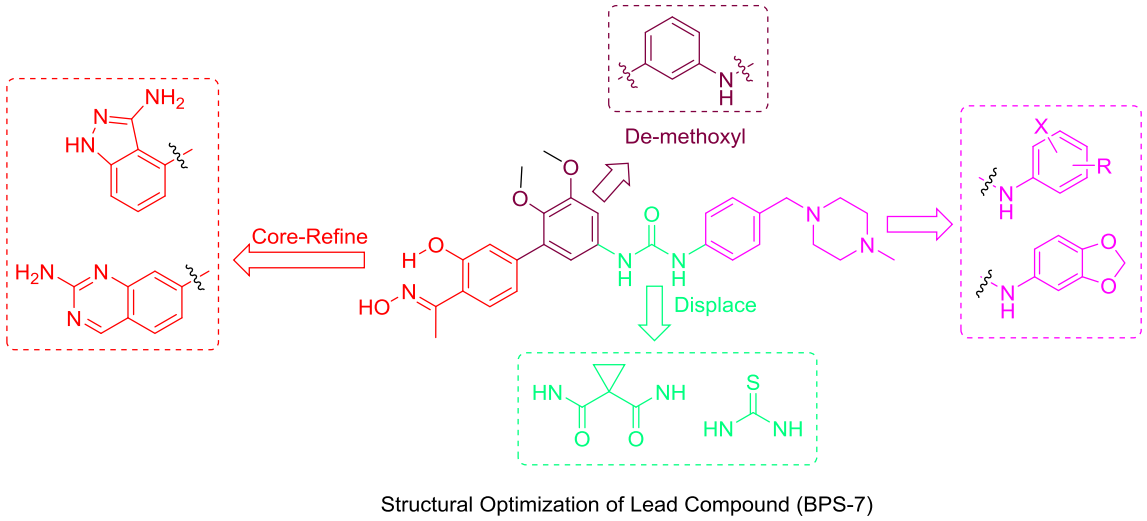

Fig. 2. Design strategies and structures of multi-targeted anti-angiogenesis agents.

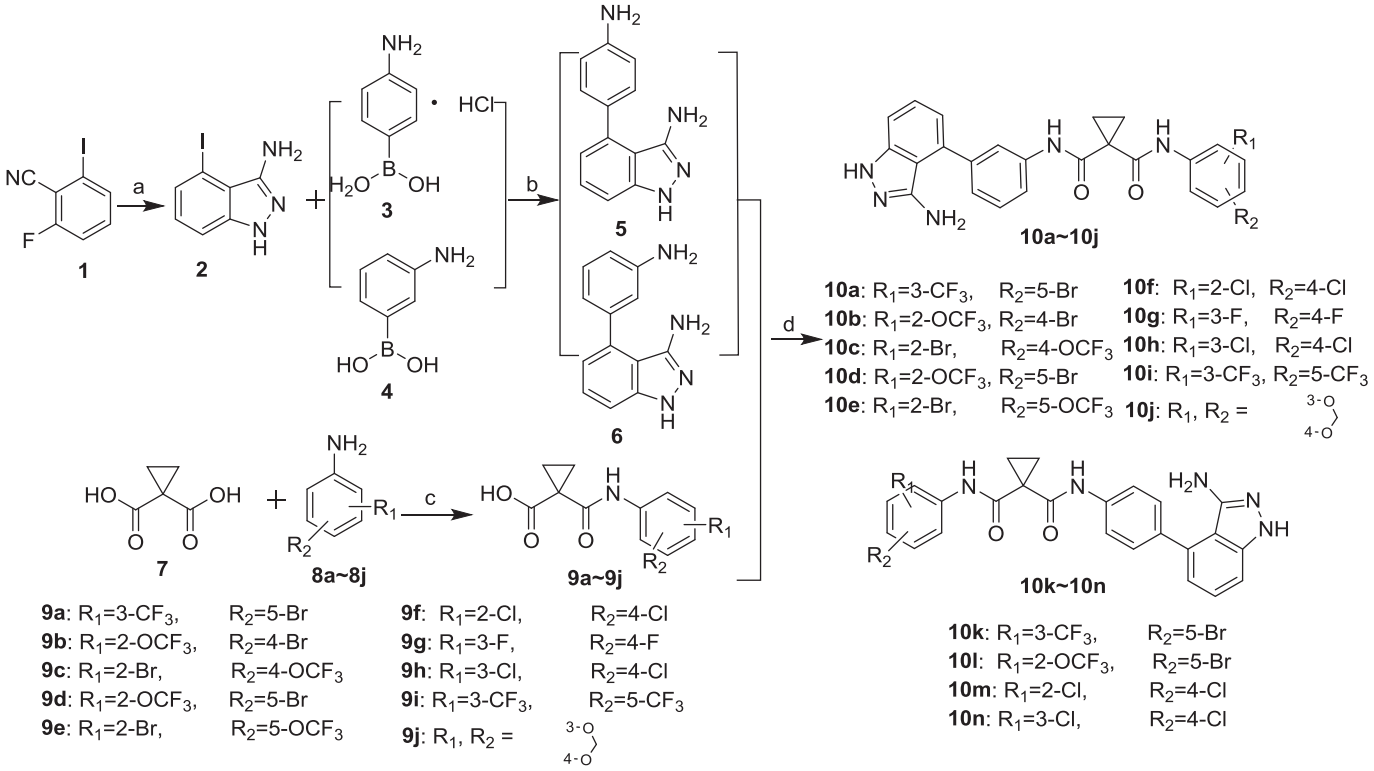

Scheme 1. Synthetic route of the title compounds (**10a~10j**).
Reagents and conditions: (**a**) EtOH, $NaHCO_3$, NH_2NH_2, H_2O; (**b**) $Pd(PPh_3)_4$, Na_2CO_3, H_2O, dioxane; (**c**) $SOCl_2$, Et_3N, DCM; (**d**) HATU, Et_3N, DCM, 0 °C to r.t.

inhibition against EphB4 with IC_{50} value of 0.13 nM. Compound (**10i**) displayed the highest VEGFR-2 inhibitory activity with IC_{50} value of 1.35 nM while compound (**10k**) was the most potent Tie-2 inhibitor with IC_{50} value of 1.95 nM.

As observed in Table 2, the majority of diaryl thioureas displayed potent and selective inhibition against Tie-2. Interestingly, four compounds (**18a**, **18b**, **18c**, and **18d**) exhibited promising multiplex inhibitory activity against VEGFR-2, Tie-2, and EphB4. These compounds bearing with trifluoromethoxy displayed more potent RTK inhibitory activity which suggested that trifluoromethoxy might be beneficial for RTK inhibition. The most potent compound (**18a**) inhibited VEGFR-2, Tie-2, and EphB4 with IC_{50} values of 1.05 nM, 2.47 nM, and 0.27 nM, respectively. These results suggested that aminoquinazoline could be considered as a novel and useful pharmacophore in the design of multi-targeted RTK inhibitors. The biological results indicated that these diaryl thioueas could be considered as the first class of multiplex inhibitors of VEGFR-2/TIE-2/EphB4 with a "triplet" inhibition profile.

2.3. Cell growth inhibition

On the basis of RTK inhibition assay, several potent compounds

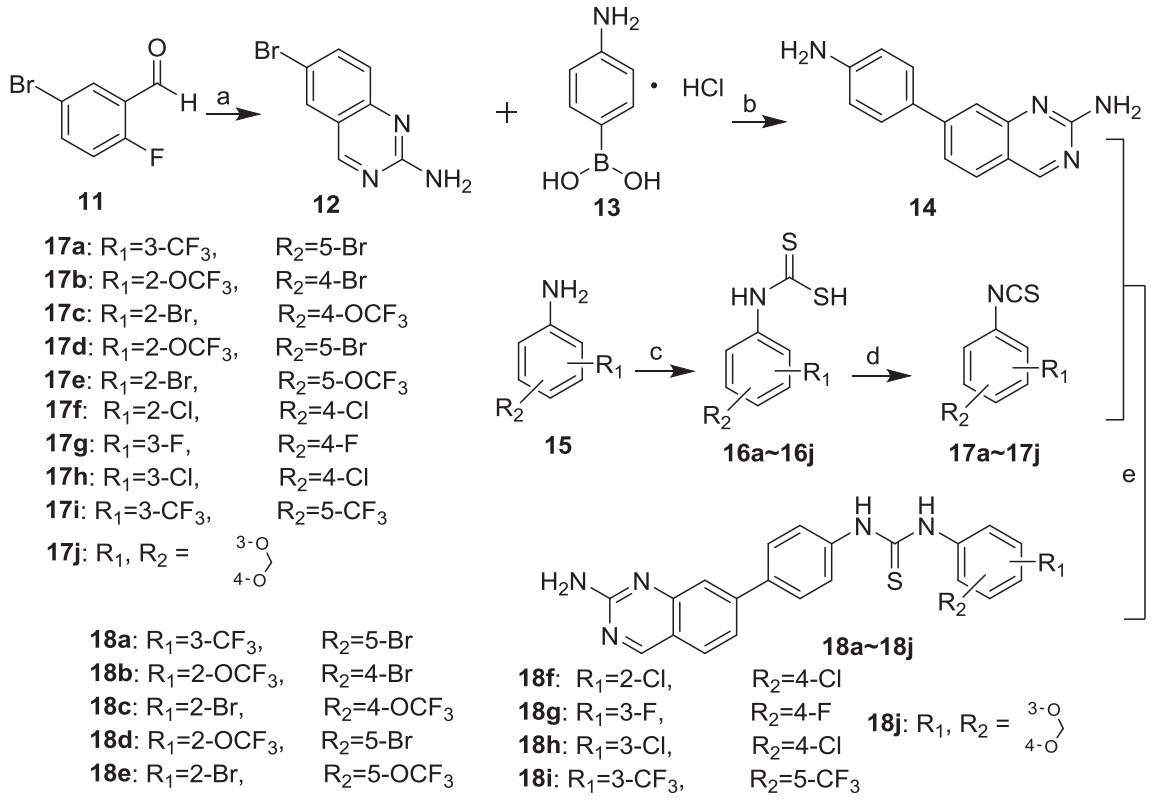

Scheme 2. Synthetic route of the title compounds (**18a~18j**).
Reagents and conditions: (**a**) guanidine carbonate, DMA, 140 °C; (**b**) $Pd(PPh_3)_4$, Na_2CO_3, H_2O, dioxane; (**c**) Dabco, CS_2, toluene; (**d**) BTC, DCM; (**e**) DCM, r.t.

Table 1
Structures and RTK inhibitory activities of title compounds (**10a-10n**) (IC_{50}, nM).

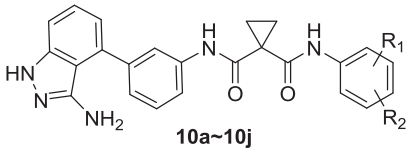

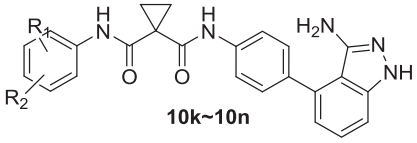

Compound	R_1	R_2	VEGFR-2	TIE-2	EphB4
10a	3-CF_3	5-Br	34.67	13.22	9.22
10b	2-OCF_3	4-Br	5.58	134.12	4.53
10c	2- Br	4-OCF_3	>1000	>1000	3.60
10d	2-OCF_3	5-Br	35.75	6.05	ND
10e	2-Br	5-OCF_3	ND	904.52	787.89
10f	2-Cl	4-Cl	7.80	>1000	383.59
10g	3-F	4-F	1.40	23.78	0.13
10h	3-Cl	4-Cl	700.53	3.49	170.11
10i	3-CF_3	5-CF_3	1.35	49.97	38.14
10j	3-O, 4-O	3-O, 4-O	>1000	6.72	1.26
10k	3-CF_3	5-Br	>1000	1.95	613.00
10l	2-OCF_3	5-Br	32.37	6.34	>1000
10m	2-Cl	4-Cl	>1000	>1000	>1000
10n	3-Cl	4-Cl	ND	>1000	>1000
Sorafinib			0.45	0.83	0.20

ND = Not Determined.

Table 2
Structures and RTK inhibitory activities of title compounds (18a-18j) (IC50, nM).

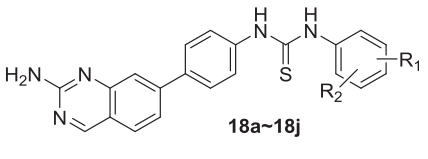

Compound	R_1	R_2	VEGFR-2	TIE-2	EphB4
18a	3-CF_3	5-Br	1.05	2.47	0.27
18b	2-OCF_3	4-Br	1.42	15.68	ND
18c	2-Br	4-OCF_3	0.31	9.68	48.53
18d	2-OCF_3	5-Br	11.41	0.60	92.59
18e	2-Br	5-OCF_3	33.02	87.38	>1000
18f	2-Cl	4-Cl	>1000	164.35	>1000
18g	3-F	4-F	>1000	52.04	>1000
18h	3-Cl	4-Cl	>1000	1.14	179.60
18i	3-CF_3	5-CF_3	>1000	0.16	ND
18j	3-O, 4-O	3-O, 4-O	>1000	0.13	ND
Sorafinib			0.45	0.83	0.20

ND = Not Determined.

were screened for their antiproliferative potency against human umbilical vein endothelial cells (EA.hy926) *in vitro*. Cell proliferation was assessed using 3-(4,5-dimethylthiazol-2-yl)-2,5-diphenyltetrazolium bromide (MTT) method with Sorafenib as positive control.

As depicted in Table 3, it was found that five of selected compounds (**10d**, **10j**, **18a**, **18c** and **18i**) displayed potent antiproliferative activities with IC_{50} values ranging from 2.68 to 7.56 μM. Their potency were comparable with the reference drug Sorafenib. Particularly, **18i** showed the highest antiproliferative activity with IC_{50} values of 2.68 μM. The antiproliferative activity was mostly in accordance with their enzymatic inhibition against

Table 3
Antiproliferative activities of title compounds against human umbilical vein endothelial cells (IC_{50}, μM).

Compound	Ea.HY926	Compound	Ea.HY926
Sorafinib	24.36	10j	4.37
10a	17.40	18a	7.56
10b	30.22	18b	25.86
10d	4.88	18c	6.58
10g	42.11	18d	336.28
10h	13.86	18i	2.68
10i	230.53	18j	ND

VEGFR-2, Tie-2, or EphB4. In summary, compound (**18a**) was a promising potent anti-angiogenesis agent and worth of further investigation.

2.4. Molecular docking study

In order to investigate the interactions between inhibitors with corresponding RTKs, docking studies were performed using Surflex-Dock Module of Sybyl-X (Version 2.0, Tripos Inc. St. Louis, MO). The most potent compound (**18a**) was drawn with Sketch module and minimized under Tripos Force field. The ligand of protein-ligand complex was used to define the binding cavity and generate the protomol [19].

The most reasonable binding configuration of (**18a**) with three RTKs were carried out and depicted in Fig. 3, Fig. 4, and Fig. 5. It was nicely bound to VEGFR-2 and presented the similar binding conformation with Sorafenib which was displayed as purple (Fig. 3). The two nitrogen atoms of thiourea unit formed two hydrogen bonds with Asp 1046 with distance of 2.38 Å and 1.96 Å, respectively. Favorable binding interactions of (**18a**) with the active site of Tie-2 including three hydrogen bonds (Fig. 4): 1) the first forming between NH_2 of aminoquinazoline and C=O of Ala 905, the distance was 2.02 Å; 2) the second forming between nitrogen atom of aminoquinazoline and NH_2 of Ala 905 with the distance of 2.19 Å; 3) the third was observed between trifluoromethyl of (**18a**) and NH_2 of Arg 987 with the distance of 1.90 Å, which suggested that trifluoromethyl might be an important element. Therefore, these results indicated that aminoquinazoline could be considered as a favorable hinge-binding fragment of Tie-2. Moreover, trifluoromethyl was identified as a critical structural requirement. The binding mode of (**18a**) with EphB4 was similar with that of native ligand (Fig. 5). Nitrogen of aminoquinazoline forms a hydrogen bond with Thr 693 with distance of 2.13 Å. In summary, molecular docking results indicated that compound (**18a**) bound in a similar fashion with native ligands of three RTK complexes. The molecular modeling results indicated that compound (**18a**) occupied the same region in the binding sites with native ligand, which clarified the rationality of the design strategy of multi-targeted RTK inhibitors as anti-angiogenesis agents.

3. Conclusion

Multiplex inhibition of angiogenesis-related RTK pathways has provided a promising strategy in the discovery of novel anti-angiogenesis agents [20–23]. Herein, we have identified several multi-targeted inhibitors of VEGFR-2/EphB4/TIE-2 with a “triplet” inhibition profile. They might be considered as potent anti-angiogenesis agents which might be useful to prevent the resistance of single-target drugs.

The biological evaluation indicated that several title compounds bearing trifluoromethyl or trifluoromethoxyl exhibited promising inhibitory activity against three angiogenesis-related RTKs and EA.hy926 proliferation. In particular, compound (**18a**) exhibited the most potent inhibition against VEGFR-2, Tie-2, and EphB4 with IC_{50} values of 1.05 nM, 2.47 nM, and 0.27 nM, respectively. In addition to their enzymatic activities, five compounds of them displayed

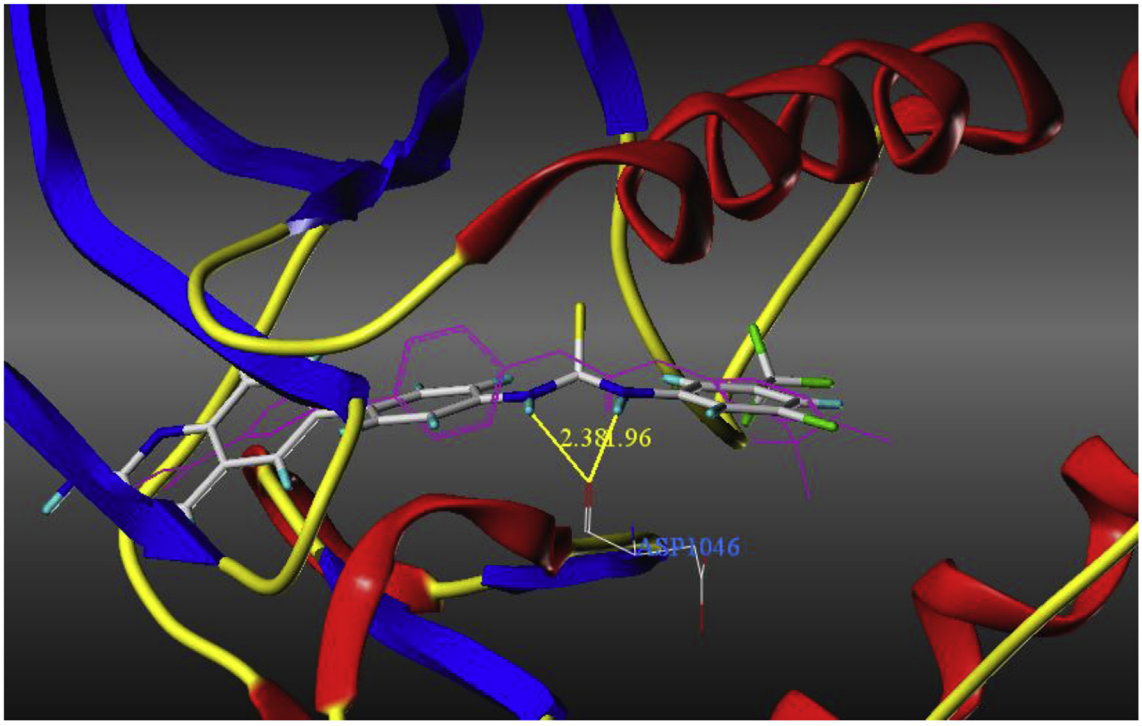

Fig. 3. Superimposition of the docking poses for VEGFR-2 with compound (18a) and Sorafenib (purple). Hydrogen bonds were depicted in dashed yellow lines. (For interpretation of the references to colour in this figure legend, the reader is referred to the web version of this article.)

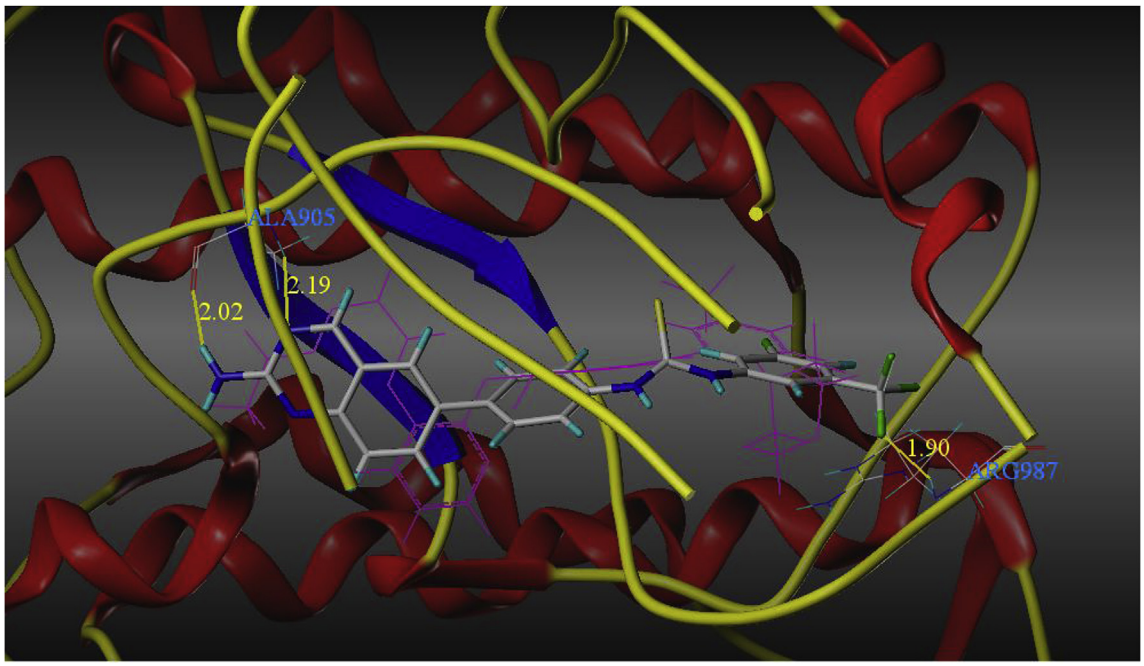

Fig. 4. Superimposition of the docking poses for Tie-2 with compound (18a) and 2-(Pyridin-2-yl)-1,3,5-triazine (purple). Hydrogen bonds were depicted in dashed yellow lines. (For interpretation of the references to colour in this figure legend, the reader is referred to the web version of this article.)

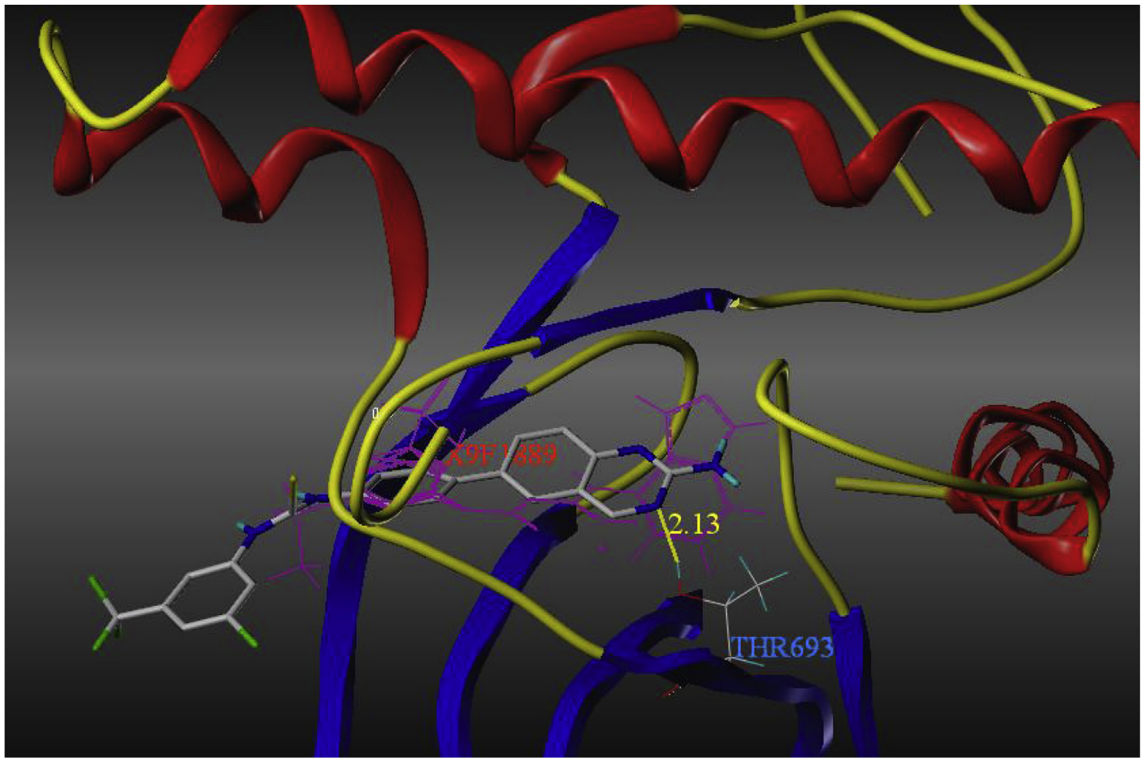

Fig. 5. Superimposition of the docking poses for EphB4 with compound (18a) and bis-anilinopyrimidine (purple). Hydrogen bonds were depicted in dashed yellow lines. (For interpretation of the references to colour in this figure legend, the reader is referred to the web version of this article.)

potent antiproliferative activity at micromolar concentrations against human umbilical vein endothelial cells (EA.hy926). Molecular docking results suggested that these novel multi-targeted inhibitors shared the similar binding conformation with native ligands of complexes. In conclusion, we disclosed our progress on identifying novel multi-targeted inhibitors. They displayed effective antiproliferative and antiangiogenic activities by targeting multiplex RTKs. Our results identified the rationality of design strategies of multi-targeted VEGFR-2, Tie-2, and EphB4 inhibitors as novel anti-angiogenesis agents. Among them, compound (**18a**)

could be considered as a promising starting point for further optimization. Our findings may contribute to the discovery of novel anti-angiogenesis agents for the intervention of pathological angiogenesis-related diseases. Further biological evaluation and structural optimization of these promising anti-angiogenesis agents are currently under investigation and will be reported in due course.

4. Experimental section

4.1. Chemistry:General procedure

The reactions except those in aqueous media are carried out by standard techniques for the exclusion of moisture. Reaction progress was monitored by thin layer chromatography (TLC) on 0.25-mm silica gel plates (60 GF-254) and visualized with UV light. Column chromatography was performed with silica gel. Melting points (mp.) are determined on electrothermal melting point apparatus and are uncorrected. ^{13}C-NMR and ^{1}H-NMR spectra are measured at 400 MHz on a Bruker Advance AC 400 instrument with TMS as an internal standard. Mass spectra are obtained on a Shimadzu HPLC-MS-QP2010 instrument.

4.1.1. 4-Iodine -1H-indazol-3-ylamine (2)

2-Fluoro-6-iodobenzonitrile was dissolved in ethanol (70 mL), then hydrazine hydrate (12.5 mL), $NaHCO_3$ (5.2 g) was added. The resulting mixture was heated to reflux and stirred for 8 h. After cooling to room temperature, 50 mL water was added and the reaction mixture was allowed to stir for another 2 h at room temperature. The product was collected by filtration and dried under vacuum to afford 4-iodine -1H-indazol-3-ylamine (2) as slight yellow solid (8 g, 77%).

4.1.2. 4-(4-minophenyl)-1H-indazol-3-amine (5)

$Pd(PPh_3)_4$ (3.3 g, 2.89 mmol) was added to a degassed solution of 4-aminophenylboronic acid (5 g, 28.9 mmol), K_2CO_3 (9.2 g, 86.7 mmol), 4-iodine -1H-indazol-3-ylamine (2) (7.5 g, 28.9 mmol) in 150 mL 1,4- dioxane and 50 mL water.The reaction mixture was heated at 90 °C in an oil bath and stirred under nitrogen for 24 h. The mixture was dissolved in H_2O and then extracted with ethyl acetate (30 mL × 3). The combined organic layer was washed with brine, dried over Na_2SO_4 for overnight, filtered, and concentrated *in vacuo* to give the crude product, which was isolated by silica gel flash chromatography (PE/AcOEt = 3:1)to obtain the title compound 3.2 g in 45% yield.

4.1.3. 1-({[3-Bromo-5-(trifluoromethyl)phenyl]amino} carbonyl) cyclopropanecarboxylic acid (9a)

1,1-Cyclopropanedicarboxylic acid (2 g, 15.4 mmol) was dissolved in anhydrous CH_2Cl_2, anhydrous triethylamine (2.2 mL) was added under nitrogen. The mixture was stirred on the ice-bath for 30 min. Thionyl chloride (1.2 mL) in anhydrous CH_2Cl_2 was added dropwise to the above mixture and stirring for 2 h. 5-bromo-3-(trifluoromethyl)-benzenamine (3.6 g, 15.4 mmol)dissolved in anhydrous CH_2Cl_2 was added into the mixture. Stirring was continued for 2 h and the solution was adjusted to pH 10 with NaOH (2 mol/L), after filtration and concentration *in vacuo*, an appropriate amount of water was added to the residues.The product was extracted with ethyl acetate (50 mL), The organic layer was separated and the aqueous layer was adjusted to pH 2 with HCl (2 mol/L). The product was extracted with ethyl acetate (50 mL × 3) again. The combined organic layer was concentrated *in vacuo*, total yielding 1-[[(3,5-dimethylphenyl)amino]carbonyl] (9) (0.8 g, 37%).

4.1.4. N-[4-(3-amino-1H-indazol-4-yl)phenyl]-N-[3-bromo-5-(trifluoromethyl)phenyl]cyclopropane-1,1-dicarboxamide (10a)

4-(4-aminophenyl)-1*H*-indazol-3-amine (5) (0.38 g, 0.7 mmol), intermediate (9a) was dissolved in anhydrous CH_2Cl_2 on the ice bath and HATU (0.48 g, 1.26 mmol) was added. The mixture was stirred on the ice-bath for 30 min, then 0.1 mL anhydrous triethylamine in anhydrous CH_2Cl_2 was added dropwise to the above mixture. Subsequently, the ice bath was removed, and the mixture was reacted at room temperature for 8 h. The product was extracted with CH_2Cl_2 (30 mL × 3), washed with water and brine (100 mL × 3), and dried over Na_2SO_4. After filtration and concentration *in vacuo*, the residues was purified by silica gel flash chromatogrphy gave (10a) (0.12 g, 20%). m.p. = 186–188 °C, TLC ($CHCl_2$:MeOH, 80:20 v/v): R_f = 0.35, MS (ESI) [M+H]+: *m/z* = 558.35. ^{1}H NMR (400 MHz, $CDCl_3$) δ 8.32 (d, *J* = 8.3 Hz, 2H), 7.55 (m, 1H, Ar-*H*), 7.33–7.14 (m, 4H, Ar-*H*), 7.11 (d, *J* = 8.5 Hz, 1H, Ar-*H*), 6.85 (m, 2H, Ar-*H*), 4.54 (d, *J* = 4.9 Hz, 2H), 1.73–1.58 (m, 4H). ^{13}C NMR (101 MHz, $CDCl_3$) δ 172.93, 171.05, 157.21, 151.17, 144.64, 142.25, 141.19, 135.75, 133.97, 133.75, 131.54, 131.25, 130.21, 129.98, 125.81, 124.20, 120.96, 119.16, 118.03, 36.99, 19.21.

Title compounds **10b**~**10j** were prepared by using the general procedure described above.

4.1.5. N-[4-(3-amino-1H-indazol-4-yl)phenyl]-N-[4-bromo-2-(trifluoromethoxy)phenyl]cyclopropane-1,1-dicarboxamide (10b)

m.p. = 96–98 °C, TLC ($CHCl_2$:MeOH, 80:20 v/v): R_f = 0.30, MS (ESI) [M+H]+: *m/z* = 574.30. ^{1}H NMR (400 MHz, $CDCl_3$) δ 8.58 (s, 1H), 8.38 (d, *J* = 8.3 Hz, 1H), 8.27 (d, *J* = 8.9 Hz, 1H), 7.57 (m,1H, Ar-*H*), 7.39 (m, 1H, Ar-*H*), 7.24 (d, *J* = 8.1 Hz, 2H, Ar-*H*), 7.19 (d, *J* = 7.3 Hz, 1H, Ar-*H*), 6.81 (d, *J* = 8.1 Hz, 2H, Ar-*H*), 4.32 (s, 2H), 1.72 (s, 4H). ^{13}C NMR (101 MHz, $CDCl_3$) δ 167.94, 167.19, 152.81, 146.76, 140.95, 138.28, 136.87, 130.55, 130.27, 130.24, 130.01, 127.61, 126.09, 123.52, 123.24, 116.87, 115.54, 115.06, 114.56, 33.33, 16.04.

4.1.6. N-[4-(3-amino-1H-indazol-4-yl)phenyl]-N-[2-bromo-4-(trifluoromethoxy)phenyl]cyclopropane-1,1-dicarboxamide(10c)

m.p. = 162–164 °C, TLC ($CHCl_2$:MeOH, 80:20 v/v): R_f = 0.28, MS (ESI) [M+H]+: *m/z* = 574.35. ^{1}H NMR (400 MHz, $CDCl_3$) δ 8.40 (d, *J* = 8.2 Hz, 1H), 8.29 (d, *J* = 9.1 Hz, 1H), 8.24 (s, 1H), 7.60–7.54 (m, 1H, Ar-*H*), 7.35 (d, *J* = 2.1 Hz, 1H, Ar-*H*), 7.25 (d, *J* = 8.3 Hz, 2H, Ar-*H*), 7.21–7.19 (m, 2H, Ar-*H*), 6.81 (d, *J* = 8.3 Hz, 2H), 4.34 (s, 2H), 1.75–1.71 (m, 2H), 1.71–1.67 (m, 2H). ^{13}C NMR (101 MHz, $CDCl_3$) δ 168.15, 167.04, 152.77, 146.66, 144.66, 140.95, 136.87, 134.98, 130.21, 130.06, 127.65, 126.06, 124.98, 122.81, 121.01, 117.03, 115.15, 114.45, 113.23, 33.42, 15.77.

4.1.7. N-[4-(3-amino-1H-indazol-4-yl)phenyl]-N-[5-bromo-2-(trifluoromethoxy)phenyl]cyclopropane-1,1-dicarboxamide(10d)

m.p. = 188–190 °C, TLC ($CHCl_2$:MeOH, 80:20 v/v): R_f = 0.32, MS (ESI) [M+H]+: *m/z* = 574.35. ^{1}H NMR (400 MHz, $CDCl_3$) δ 8.65 (s, 1H), 8.60 (d, *J* = 2.2 Hz, 1H), 8.37 (d, *J* = 8.3 Hz, 1H), 7.58–7.52 (m, 1H, Ar-*H*), 7.23 (d, *J* = 8.3 Hz, 2H, Ar-*H*), 7.19 (d, *J* = 3.4 Hz, 1H, Ar-*H*), 7.04 (m, 1H, Ar-*H*), 6.79 (d, *J* = 8.3 Hz, 2H, Ar-*H*), 4.35 (s, 2H), 1.73 (s, 4H). ^{13}C NMR (101 MHz, $CDCl_3$) δ 171.21, 168.02, 167.15, 152.85, 146.84, 140.94, 136.90, 132.22, 130.21, 130.00, 127.54, 126.73, 126.08, 124.87, 121.62, 120.72, 116.88, 115.04, 114.53, 33.27, 16.18.

4.1.8. N-[4-(3-amino-1H-indazol-4-yl)phenyl]-N-[2-bromo-5-(trifluoromethoxy)phenyl]cyclopropane-1,1-dicarboxamide(10e)

m.p. = 156–157 °C, TLC ($CHCl_2$:MeOH, 80:20 v/v): R_f = 0.40, MS (ESI) [M+H]+: *m/z* = 574.35. ^{1}H NMR (400 MHz, $CDCl_3$) δ 8.41 (d, *J* = 8.1 Hz, 1H), 8.34 (s, 1H), 8.31 (d, *J* = 2.4 Hz, 1H), 7.60–7.54 (m, 1H, Ar-*H*), 7.45 (d, *J* = 8.8 Hz, 1H, Ar-*H*), 7.24 (d, *J* = 8.4 Hz, 2H, Ar-*H*), 7.20 (d, *J* = 7.1 Hz, 1H, Ar-*H*), 6.80 (d, *J* = 8.4 Hz, 2H, Ar-*H*), 4.34 (s, 2H), 1.75 (m, 2H), 1.70 (m, 2H). ^{13}C NMR (101 MHz, $CDCl_3$) δ 168.20,

166.94, 152.84, 148.73, 148.71, 146.82, 140.96, 137.18, 136.94, 132.74, 130.22, 130.04, 127.51, 126.08, 117.05, 115.08, 114.81, 114.43, 110.44, 33.48, 15.93.

4.1.9. N-[4-(3-amino-1H-indazol-4-yl)phenyl]-N-(2,4-dichlorophenyl)cyclopropane-1,1-dicarboxamide(10f)

m.p. = 153–155 °C, TLC ($CHCl_2$:MeOH, 80:20 v/v): R_f = 0.35, MS (ESI) [M+H]+: *m/z* = 480.35. ^{1}H NMR (400 MHz, $CDCl_3$) δ 8.40 (s, 1H), 8.38 (s, 1H), 8.22 (d, *J* = 8.9 Hz, 1H), 7.57 (m, 1H, Ar-*H*), 7.30 (d, *J* = 2.4 Hz, 1H, Ar-*H*), 7.27–7.24 (m, 2H, Ar-*H*), 7.21 (d, *J* = 2.4 Hz, 1H, Ar-*H*), 6.84–6.80 (m, 2H, Ar-*H*), 4.32 (s, 2H), 1.73 (m, 2H), 1.68 (m, 2H). ^{13}C NMR (101 MHz, $CDCl_3$) δ 167.96, 167.12, 152.71, 146.61, 140.95, 136.88, 133.70, 130.22, 130.07, 128.91, 128.63, 127.72, 127.68, 126.05, 123.52, 122.87, 116.91, 115.16, 114.50, 33.43, 15.75.

4.1.10. N-[4-(3-amino-1H-indazol-4-yl)phenyl]-N-(3,4-difluorophenyl)cyclopropane-1,1-dicarboxamide (10g)

m.p. = 105–107 °C, TLC ($CHCl_2$:MeOH, 80:20 v/v): R_f = 0.30, MS (ESI) [M+H]+: *m/z* = 447.45. ^{1}H NMR (400 MHz, DMSO) δ 9.86 (s, 1H), 8.25 (d, *J* = 8.2 Hz, 1H), 7.69 (d, *J* = 3.8 Hz, 1H, Ar-*H*), 7.56 (m, 1H, Ar-*H*), 7.29 (d, *J* = 9.0 Hz, 1H, Ar-*H*), 7.26 (s, 1H, Ar-*H*), 7.11 (m, 3H, Ar-*H*), 6.70 (d, *J* = 8.4 Hz, 2H), 5.13 (s, 2H), 1.51 (m, 2H), 1.45 (m, 2H). ^{13}C NMR (101 MHz, DMSO) δ 168.12, 167.27, 152.31, 149.11, 140.73, 137.65, 136.87, 136.78, 130.00, 125.57, 125.04, 117.46, 117.29, 117.06, 116.90, 114.43, 113.98, 110.02, 109.81, 33.07, 14.60.

4.1.11. N-[4-(3-amino-1H-indazol-4-yl)phenyl]-N-(3,4-dichlorophenyl)cyclopropane-1,1-dicarboxamide (10h)

m.p. = 103–104 °C, TLC ($CHCl_2$:MeOH, 80:20 v/v): R_f = 0.25, MS (ESI) [M+H]+: *m/z* = 480.35. ^{1}H NMR (400 MHz, DMSO) δ 9.95 (s, 1H), 8.26 (d, *J* = 8.1 Hz, 1H), 7.91 (s, 1H, Ar-*H*), 7.59–7.54 (m, 1H, Ar-*H*), 7.49 (s, 2H, Ar-*H*), 7.12 (d, *J* = 8.2 Hz, 3H, Ar-*H*), 6.73 (d, *J* = 8.4 Hz, 2H), 5.12 (s, 2H), 1.53 (m, 2H), 1.46 (m, 2H). ^{13}C NMR (101 MHz, $CDCl_3$) δ 168.29, 167.14, 152.33, 148.68, 140.72, 139.98, 137.60, 131.10, 130.71, 130.03, 125.60, 125.36, 124.95, 121.92, 120.69, 116.90, 114.68, 114.02, 33.16, 14.73.

4.1.12. N-[4-(3-amino-1H-indazol-4-yl)phenyl]-N-[3,5-bis(trifluoromethyl)phenyl]cyclopropane-1,1-dicarboxamide (10i)

m.p. = 135–137 °C, TLC ($CHCl_2$:MeOH, 80:20 v/v): R_f = 0.30, MS (ESI) [M+H]+: *m/z* = 547.45. ^{1}H NMR (400 MHz, $CDCl_3$) δ 9.27 (s, 1H), 8.18 (d, *J* = 8.3 Hz, 1H), 8.06 (s, 2H), 7.56 (s, 1H, Ar-*H*), 7.44–7.38 (m, 1H, Ar-*H*), 7.23 (d, *J* = 8.4 Hz, 2H, Ar-*H*), 7.15–7.11 (m, 1H, Ar-*H*), 6.81 (d, *J* = 8.4 Hz, 2H), 4.33 (s, 2H), 1.74 (d, *J* = 3.1 Hz, 2H), 1.71 (d, *J* = 3.1 Hz, 2H). ^{13}C NMR (101 MHz, $CDCl_3$) δ 168.41, 167.58, 165.70, 152.67, 146.68, 140.91, 140.12, 136.96, 132.25, 131.92, 130.00, 127.53, 126.06, 124.53, 121.82, 119.82, 117.02, 116.85, 115.17, 114.36, 33.06, 15.97.

4.1.13. N-[4-(3-amino-1H-indazol-4-yl)phenyl]-N-1,3-benzodioxol-5-ylcyclopropane-1,1-dicarboxamide (10j)

m.p. = 116–118 °C, TLC ($CHCl_2$:MeOH, 80:20 v/v): R_f = 0.38, MS (ESI) [M+H]+: *m/z* = 455.45. ^{1}H NMR (400 MHz, $CDCl_3$) δ 8.28 (d, *J* = 7.4 Hz, 1H), 8.08 (s, 1H), 7.47 (m, 1H, Ar-*H*), 7.24 (d, *J* = 8.2 Hz, 2H, Ar-*H*), 7.15 (d, *J* = 7.1 Hz, 2H, Ar-*H*), 6.79 (d, *J* = 8.2 Hz, 2H, Ar-*H*), 6.70 (d, *J* = 11.8 Hz, 1H), 5.90 (s, 2H), 4.39 (s, 2H), 1.67 (s, 2H), 1.60 (s, 2H). ^{13}C NMR (101 MHz, $CDCl_3$) δ 167.85, 152.53, 147.65, 146.82, 144.23, 140.87, 136.90, 132.44, 130.06, 127.56, 125.91, 120.63, 116.87, 115.06, 114.41, 113.70, 107.91, 103.43, 101.17, 38.63, 33.08, 15.18.

4.1.14. 4-(4-aminophenyl)-1H-indazol-3-amine (6)

$Pd(PPh_3)_4$ (3.4 g, 3.65 mmol) was added to a degassed solution of 3-aminobenzeneboronic acid (4 g, 36.5 mmol), K_2CO_3 (9.3 g, 87.6 mmol), 4-iodine -1H-indazol-3-ylamine (2) (7.6 g, 36.5 mmol) in 150 mL 1,4-dioxane and 50 mL water. The reaction mixture was heated at 90 °C in an oil bath and stirred under nitrogen for 24 h. The mixture was dissolved in H_2O and then extracted with ethyl acetate (30 mL × 3). The combined organic layer was washed with brine, dried over Na_2SO_4 for overnight, filtered, and concentrated *in vacuo* to give the crude product, which was isolated by silica gel flash chromatography (PE/AcOEt = 3:1) to obtain the title compound 2.9 g with yield of 40%.

4.1.15. 1-[[(3,5-dimethylphenyl)amino]carbonyl] (9)

1,1-cyclopropanedicarboxylic acid (2 g, 15.4 mmol) was dissolved in anhydrous CH_2Cl_2 (15 mL), anhydrous triethylamine (2.2 mL) was added under nitrogen atmosphere, the mixture was stirred on the ice-bath for 30 min. Thionyl chloride (1.2 mL) in anhydrous CH_2Cl_2 (10 mL) was added dropwise to the above mixture and stirring continued for 2 h. 3-bromo-5-(trifluoromethyl)-benzenamine (3.5 g, 13.9 mmol) dissolved in anhydrous CH_2Cl_2 was then added into the mixture. Stirring was continued for 2 h and the solution was adjusted to pH 10 with NaOH (2 mol/L), after filtration and concentration *in vacuo*, an appropriate amount of water was added to the residues. The product was extracted with ethyl acetate (50 mL). The organic layer was separated and the aqueous layer was adjusted to pH 2 with HCl (2 mol/L) The product was extracted with ethyl acetate (50 mL × 3) The combined organic layer was concentrated *in vacuo*, total yielding (9) (0.8 g, 35%).

4.1.16. N-[3-(3-amino-1H-indazol-4-yl)phenyl]-N-[3-bromo-5-(trifluoromethyl)phenyl]cyclopropane-1,1-dicarboxamide (10k)

Compound (6) (0.38 g, 0.7 mmol), 1-[[(3,5-dimethyl phenyl) amino]carbonyl] (0.34 g, 0.92 mmol) was dissolved in anhydrous CH_2Cl_2 (10 mL), and HATU (0.63 g,1.66 mmol) was added, the mixture was stirred on the ice-bath for 30 min, then 0.13 mL anhydrous triethylamine in anhydrous CH_2Cl_2 was slowly added dropwise to the above mixture, after that, the ice bath was removed, and the mixture was reacted at room temperature for 8 h. The product was extracted with CH_2Cl_2 (30 mL × 3), washed with water and brine (100 mL × 3), and dried over Na_2SO_4. After filtration and concentration *in vacuo*, the residues was purified by silica gel flash chromatogrphy gave (10k) (0.12 g, 25%). m.p. = 171–173 °C, TLC ($CHCl_2$:MeOH, 80:20 v/v): R_f = 0.23, MS (ESI) [M+H]+: *m/z* = 558.35. ^{1}H NMR (400 MHz, $CDCl_3$) δ 8.64–8.59 (m, 2H), 8.42 (d, *J* = 8.3 Hz, 1H), 7.61–7.54 (m, 1H, Ar-*H*), 7.31–7.25 (m, 1H, Ar-*H*), 7.22 (d, *J* = 7.3 Hz, 1H, Ar-*H*), 7.04 (m, 1H, Ar-*H*), 6.83–6.77 (m, 2H), 6.74 (s, 1H), 4.38 (s, 2H), 1.73 (s, 4H). ^{13}C NMR (101 MHz, $CDCl_3$) δ 167.97, 167.21, 152.63, 146.63, 140.85, 139.00, 136.96, 136.77, 132.21, 130.18, 129.75, 126.74, 125.75, 124.83, 121.65, 120.77, 118.97, 116.65, 115.41, 115.10, 115.06, 33.28, 16.19.

Title compounds **10l**~**10n** were prepared by using the general procedure described above.

4.1.17. N-[3-(3-amino-1H-indazol-4-yl)phenyl]-N-[5-bromo-2-(trifluoromethoxy)phenyl]cyclopropane-1,1-dicarboxamide (10l)

m.p. = 173–174 °C, TLC ($CHCl_2$:MeOH, 80:20 v/v): R_f = 0.27, MS (ESI) [M+H]+: *m/z* = 574.35. ^{1}H NMR (400 MHz, $CDCl_3$) δ 8.62 (s, 1H), 8.61 (d, *J* = 2.3 Hz, 1H), 8.41 (d, *J* = 8.1 Hz, 1H), 7.60–7.55 (m, 1H, Ar-*H*), 7.31–7.26 (m, 1H, Ar-*H*), 7.22 (d, *J* = 6.9 Hz, 1H, Ar-*H*), 7.04 (m, 1H, Ar-*H*), 6.79 (m, 2H), 6.74 (d, *J* = 1.7 Hz, 1H), 4.38 (s, 2H), 1.73 (s, 4H). ^{13}C NMR (101 MHz, $CDCl_3$) δ 167.97, 167.21, 152.64, 146.72, 140.84, 139.00, 136.97, 136.79, 132.21, 130.17, 129.75, 126.74, 125.75, 124.83, 121.65, 121.44, 120.76, 118.90, 116.65, 115.36, 115.05, 33.28, 16.19.

4.1.18. N-[3-(3-amino-1H-indazol-4-yl)phenyl]-N-(2,4-dichlorophenyl)cyclopropane-1,1-dicarboxamide (10m)

m.p. = 109–111 °C, TLC ($CHCl_2$:MeOH, 80:20 v/v): R_f = 0.25, MS

(ESI) [M+H]+: m/z = 480.35. ^{1}H NMR (400 MHz, $CDCl_3$) δ 8.43 (d, J = 8.3 Hz, 1H), 8.38 (s, 1H), 8.22 (d, J = 8.8 Hz, 1H), 7.59 (m, 1H, Ar-*H*), 7.30–7.28 (m, 3H, Ar-*H*), 7.25–7.20 (m, 2H, Ar-*H*), 6.82 (d, J = 7.6 Hz, 1H, Ar-*H*), 6.77 (d, J = 9.7 Hz, 1H), 4.37 (s, 2H), 1.72 (s, 2H), 1.69 (s, 2H). ^{13}C NMR (101 MHz, $CDCl_3$) δ 167.94, 167.16, 152.49, 146.58, 140.84, 138.98, 136.78, 133.68, 130.16, 129.76, 128.93, 128.63, 127.74, 125.72, 122.83, 119.06, 116.69, 115.47, 115.12, 115.02, 38.63, 33.43.

4.1.19. N-[3-(3-amino-1H-indazol-4-yl)phenyl]-N-[3,5-bis(trifluoromethyl)phenyl]cyclopropane-1,1-dicarboxamide (10n)

m.p. = 112–114 °C, TLC ($CHCl_2$:MeOH, 80:20 v/v): R_f = 0.24, MS (ESI) [M+H]+: m/z = 547.45. ^{1}H NMR (400 MHz, $CDCl_3$) δ 9.18 (s, 1H), 8.13 (d, J = 8.3 Hz, 1H), 8.06 (s, 2H), 7.57 (s, 1H, Ar-*H*), 7.35 (m, 1H, Ar-*H*), 7.28 (m, 1H, Ar-*H*), 7.13 (d, J = 7.3 Hz, 1H, Ar-*H*), 6.80 (d, J = 7.7 Hz, 2H), 6.72 (s, 1H), 4.40 (s, 2H), 1.76 (d, J = 9.7 Hz, 2H), 1.71 (d, J = 9.7 Hz, 2H). ^{13}C NMR (101 MHz, $CDCl_3$) δ 168.28, 167.76, 152.62, 146.55, 140.73, 139.99, 138.78, 136.85, 132.33, 132.00, 130.01, 129.84, 125.85, 124.50, 121.78, 119.74, 119.01, 116.67, 115.39, 115.26, 114.79, 33.09, 16.03.

4.1.20. 6-Bromo-2-quinazolinamine (12)

Compound 2-Fluoro-5-bromobenzaldehyde (10.0 g, 49.2 mmol) bisguanidiniu carbonate (13.3 g, 74 mmol) were dissolved in *N,N*-dimethylacetamide (50 mL). The resulting mixture was heated to reflux and stirred for 5 h. After cooling to room temperature, 120 mL of water was added and the reaction mixture was allowed to stir for another 2 h at room temperature. The product was collected by filtration and dried under vacuum to yield 6-Bromo-2-quinazolinamine (12) (5 g, 60%).

4.1.21. 7-(4-Aminophenyl)- 2-quinazolinamine (14)

$Pd(PPh_3)_4$ (1.03 g, 0.89 mmol) was added to a degassed solution of 4-aminophenylboronic acid (1.54 g, 8.9 mmol), K_2CO_3 (2.8 g, 26.7 mmol), 6-bromo-2-quinazolinamine (12) (2.0 g, 8.9 mmol) in 120 mL 1,4-dioxane and 40 mL water. The reaction mixture was heated at 100 °C in an oil bath and stirred under nitrogen for 24 h. The mixture was dissolved in H_2O and then extracted with ethyl acetate (30 mL × 3). The combined organic layer was washed with brine, dried over Na_2SO_4 for overnight, filtered, and concentrated *in vacuo* to give the crude product, which was isolated by silica gel flash chromatography (PE/AcOEt = 3:1)to obtain the title compound 0.8 g with yield of 28%.

4.1.22. (3-Bromo-5-(trifluoromethyl)phenyl) carbamodithioic acid (16)

3-bromo-5-(trifluoromethyl)aniline (11) (2.5 g, 10.4 mmol), DABC (1.4 g, 12.5 mmol) was dissolved in toluene (40 mL). Then 1.9 mL carbon disulphide was added dropwise to the above mixture, after that, the mixture was reacted at room temperature for 8 h. The product was collected by filtration and dried under vacuum to give (3-bromo-5-(trifluoromethyl)phenyl)carbamodithioic acid (16) as slight yellow solid (1.2 g, 40%).

4.1.23. 1-Bromo-3-isothiocyanato-5-(trifluoromethyl) benzene (17)

(3-bromo-5-(trifluoromethyl)phenyl)carbamodithioic acid (16) (0.8 g, 2.5 mmol) was dissolved in anhydrous CH_2Cl_2 (20 mL). Then triphosgene (0.88 g, 3 mmol) in anhydrous CH_2Cl_2 was added dropwise to the above mixture on the ice-bath. Then stirring continued for 2 h at room temperature. After completion of the reaction, the organic layer was washed with water and brine (100 mL × 3), and dried over Na_2SO_4. After filtration and concentration *in vacuo*, the residue was purified by silica gel flash chromatography, yielding (17) (0.5 g, 30%).

4.1.24. N-[4-(2-aminoquinazolin-7-yl)phenyl]-N'-[3-bromo-5-(trifluoromethyl)phenyl]thiourea (18a)

7-(4-aminophenyl)-2-quinazolinamine (9) (0.2 g, 0.85 mmol) was dissolved in anhydrous CH_2Cl_2 (10 mL). 1-bromo-3-isothiocyanato-5-(trifluoromethyl)benzene (17) (0.23 g, 0.77 mmol) in anhydrous CH_2Cl_2 (10 mL) was added dropwise to the above mixture, and stirring on the ice-bath continued for 2 h. After stirring at room temperature for 18 h. The organic layer was washed with water and brine (100 mL × 3), and dried over Na_2SO_4. After filtration and concentration *in vacuo*, the residue was purified by silica gel flash chromatography, yielding (18a) (0.12 g, 30%).

m.p. = 263–265 °C, TLC ($CHCl_2$:MeOH, 90:10 v/v): R_f = 0.32, MS (ESI) [M+H]+: m/z = 518.35. ^{1}H NMR (400 MHz, DMSO) δ 10.39 (s, 1H), 10.23 (s, 1H), 9.18 (s, 1H), 8.13 (d, J = 6.8 Hz, 2H), 8.05 (d, J = 8.7 Hz, 1H), 8.00–7.89 (m, 2H), 7.76 (d, J = 7.4 Hz, 2H, Ar-*H*), 7.69 (s, 1H, Ar-*H*), 7.59 (d, J = 7.4 Hz, 1H, Ar-*H*), 7.51 (d, J = 8.7 Hz, 1H, Ar-*H*), 6.99 (s, 2H). ^{13}C NMR (101 MHz, DMSO) δ 179.99, 163.18, 161.33, 142.61, 138.53, 136.33, 133.39, 133.27, 129.86, 127.50, 127.17, 125.57, 125.38, 124.70, 124.32, 121.99, 120.12, 119.25, 114.78.

Title compounds **18b**~**18j** were prepared by using the general procedure described above.

4.1.25. N-[4-(2-aminoquinazolin-7-yl)phenyl]-N'-[4-bromo-2-(trifluoromethoxy)phenyl]thiourea (18b)

m.p. = 257–259 °C, TLC ($CHCl_2$:MeOH, 90:10 v/v): R_f = 0.30, MS (ESI) [M+H]+: m/z = 534.35. ^{1}H NMR (400 MHz, DMSO) δ 10.24 (s, 1H), 9.62 (s, 1H), 9.18 (s, 1H), 8.12 (s, 1H), 8.06 (d, J = 8.8 Hz, 1H), 7.75 (m, 3H, Ar-*H*), 7.70 (s, 1H), 7.63 (d, J = 8.5 Hz, 3H, Ar-*H*), 7.51 (d, J = 8.8 Hz, 1H, Ar-*H*), 6.98 (s, 2H). ^{13}C NMR (101 MHz, DMSO) δ 180.67, 163.23, 161.28, 143.47, 138.82, 136.14, 133.41, 133.28, 132.18, 131.25, 130.89, 127.00, 125.51, 125.36, 124.77, 124.54, 120.11, 119.12, 118.52.

4.1.26. N-[4-(2-aminoquinazolin-7-yl)phenyl]-N'-[2-bromo-4-(trifluoromethoxy)phenyl]thiourea (18c)

m.p. = 251–253 °C, TLC ($CHCl_2$:MeOH, 90:10 v/v): R_f = 0.29, MS (ESI) [M+H]+: m/z = 534.35. ^{1}H NMR (400 MHz, DMSO) δ 10.27 (s, 1H), 9.59 (s, 1H), 9.18 (s, 1H), 8.12 (s, 1H), 8.06 (d, J = 8.8 Hz, 1H), 7.80 (s, 1H, Ar-*H*), 7.76 (d, J = 8.5 Hz, 2H, Ar-*H*), 7.69 (d, J = 5.8 Hz, 2H, Ar-*H*), 7.66 (s, 1H, Ar-*H*), 7.51 (d, J = 8.8 Hz, 1H, Ar-*H*), 7.44 (d, J = 8.3 Hz, 1H, Ar-*H*), 6.98 (s, 2H). ^{13}C NMR (101 MHz, DMSO) δ 180.68, 163.25, 161.26,138.83, 138.07, 136.05, 133.44, 133.29, 131.89, 127.51, 127.02, 125.77, 125.48, 125.34, 124.57, 122.53, 121.06, 120.11, 114.82.

4.1.27. N-[4-(2-aminoquinazolin-7-yl)phenyl]-N'-[5-bromo-2-(trifluoromethoxy)phenyl]thiourea (18d)

m.p. = 253–255 °C, TLC ($CHCl_2$:MeOH, 90:10 v/v): R_f = 0.32, MS (ESI) [M+H]+: m/z = 534.35. ^{1}H NMR (400 MHz, DMSO) δ 10.32 (s, 1H), 9.67 (s, 1H), 9.18 (s, 1H), 8.13 (d, J = 1.8 Hz, 1H), 8.08–8.04 (m, 2H), 7.76 (d, J = 8.6 Hz, 2H, Ar-*H*), 7.64 (d, J = 8.5 Hz, 2H, Ar-*H*), 7.55 (m, 1H, Ar-*H*), 7.51 (d, J = 8.8 Hz, 1H, Ar-*H*), 7.42 (d, J = 8.8 Hz, 1H, Ar-*H*), 6.98 (s, 2H). ^{13}C NMR (101 MHz, DMSO) δ 180.55, 163.32, 161.21, 142.15, 138.73, 136.21, 134.03, 133.44, 133.32, 131.70, 130.00, 128.18, 127.03, 125.40, 124.58, 123.48, 120.09, 119.34,116.58.

4.1.28. N-[4-(2-aminoquinazolin-7-yl)phenyl]-N'-[2-bromo-5-(trifluoromethoxy)phenyl]thiourea (18e)

m.p. = 256–258 °C, TLC ($CHCl_2$:MeOH, 90:10 v/v): R_f = 0.35, MS (ESI) [M+H]+: m/z = 534.35. ^{1}H NMR (400 MHz, DMSO) δ 10.41 (s, 1H), 9.63 (s, 1H), 9.20 (s, 1H), 8.14 (s, 1H), 8.07 (d, J = 8.8 Hz, 1H), 7.82 (d, J = 8.8 Hz, 1H, Ar-*H*), 7.77 (d, J = 8.4 Hz, 2H, Ar-*H*), 7.73 (s, 1H, Ar-*H*), 7.69 (d, J = 8.4 Hz, 2H, Ar-*H*), 7.52 (d, J = 8.7 Hz, 1H, Ar-*H*), 7.25 (d, J = 7.0 Hz, 1H, Ar-*H*), 7.09 (s, 2H). ^{13}C NMR (101 MHz, DMSO) δ 180.32, 163.46, 161.08, 147.46, 139.94, 138.68, 136.13, 134.30, 133.53, 133.39, 127.07, 125.41, 125.26, 124.61, 122.74, 120.60, 120.07,

119.73,116.58.

4.1.29. N-[4-(2-aminoquinazolin-7-yl)phenyl]-N'-(2,4-dichlorophenyl)thiourea(18f)

m.p. = 243–245 °C, TLC ($CHCl_2$:MeOH, 90:10 v/v): R_f = 0.40, MS (ESI) [M+H]+: *m/z* = 440.35. ^{1}H NMR (400 MHz, DMSO) δ 10.25 (s, 1H), 9.62 (s, 1H), 9.19 (d, *J* = 3.9 Hz, 1H), 8.13 (d, *J* = 1.9 Hz, 1H), 8.06 (m, 1H), 7.80–7.73 (m, 2H, Ar-*H*), 7.71 (d, *J* = 2.4 Hz, 1H, Ar-*H*), 7.67 (s, 1H, Ar-*H*), 7.63 (d, *J* = 9.1 Hz, 2H, Ar-*H*), 7.52 (d, *J* = 8.8 Hz, 1H, Ar-*H*), 7.45 (m, 1H, Ar-*H*), 7.07 (s, 2H). ^{13}C NMR (101 MHz, DMSO) δ 180.65, 163.40, 161.11, 138.89, 136.19, 135.99, 133.54, 133.36, 131.74, 131.48, 131.38, 129.39, 127.84, 127.01, 125.37, 125.31, 124.54, 124.27,120.08.

4.1.30. N-[4-(2-aminoquinazolin-7-yl)phenyl]-N'-(3,4-difluorophenyl)thiourea(18g)

m.p. = 255–257 °C, TLC ($CHCl_2$:MeOH, 90:10 v/v): R_f = 0.28, MS (ESI) [M+H]+: *m/z* = 407.45. ^{1}H NMR (400 MHz, DMSO) δ 10.47 (s, 1H), 10.44 (s, 1H), 9.53 (s, 1H), 8.39 (s, 1H), 8.30 (d, *J* = 7.3 Hz, 1H), 7.77 (d, *J* = 8.6 Hz, 3H, Ar-*H*), 7.73 (s, 1H, Ar-*H*), 7.70 (d, *J* = 8.6 Hz, 2H, Ar-*H*), 7.43 (d, *J* = 10.3 Hz, 2H, Ar-*H*), 7.28 (d, *J* = 8.8 Hz, 1H, Ar-*H*). ^{13}C NMR (101 MHz, DMSO) δ 179.95, 168.70, 161.46, 139.77, 137.79, 135.82, 134.56, 132.20, 131.02, 127.19, 126.47, 124.26, 120.44, 119.22, 117.94, 117.59, 117.40, 113.23, 113.04.

4.1.31. N-[4-(2-aminoquinazolin-7-yl)phenyl]-N'-(3,4-dichlorophenyl)thiourea (18h)

m.p. = 152–154 °C, TLC ($CHCl_2$:MeOH, 90:10 v/v): R_f = 0.27, MS (ESI) [M+H]+: *m/z* = 440.35. ^{1}H NMR (400 MHz, DMSO) δ 10.62 (s, 1H), 9.44 (d, *J* = 6.4 Hz, 1H), 8.30 (s, 1H), 8.23 (d, *J* = 8.5 Hz, 2H), 8.03 (s, 1H), 7.75 (s, 1H, Ar-*H*), 7.73–7.68 (m, 2H, Ar-*H*), 7.64 (d, *J* = 8.7 Hz, 2H, Ar-*H*), 7.59 (s, 1H, Ar-*H*), 7.55 (s, 1H, Ar-*H*). ^{13}C NMR (101 MHz, DMSO) δ 179.69, 168.84, 140.27,135.22, 135.20, 130.90, 130.68, 127.91, 127.54, 127.16, 126.22, 125.71, 124.61, 124.26, 124.21, 123.48, 119.44, 118.91, 114.80.

4.1.32. N-[4-(2-aminoquinazolin-7-yl)phenyl]-N'-[3,5-bis(trifluoromethyl)phenyl]thioura(18i)

m.p. = 252–254 °C, TLC ($CHCl_2$:MeOH, 90:10 v/v): R_f = 0.35, MS (ESI) [M+H]+: *m/z* = 507.45. ^{1}H NMR (400 MHz, DMSO) δ 10.46 (s, 1H), 10.32 (s, 1H), 9.18 (s, 1H), 8.29 (s, 2H), 8.12 (d, *J* = 1.7 Hz, 1H), 8.05 (m, 1H), 7.83 (s, 1H, Ar-*H*), 7.77 (d, *J* = 8.5 Hz, 2H, Ar-*H*), 7.58 (d, *J* = 8.5 Hz, 2H, Ar-*H*), 7.51 (d, *J* = 8.8 Hz, 1H, Ar-*H*), 6.97 (s, 2H). ^{13}C NMR (101 MHz, DMSO) δ 180.13, 163.17, 161.35, 142.34, 138.37, 136.49, 133.34, 133.26, 130.62, 130.29, 127.24, 125.61, 125.41, 124.82, 124.00, 122.37, 120.12, 119.62, 118.29.

4.1.33. N-[4-(2-aminoquinazolin-7-yl)phenyl]-N'-1,3-benzodioxol-5-ylthiourea(18j)

m.p. = 230–231 °C, TLC ($CHCl_2$:MeOH, 90:10 v/v): R_f = 0.33, MS (ESI) [M+H]+: *m/z* = 415.45. ^{1}H NMR (400 MHz, DMSO) δ 9.82 (s, 1H), 9.77 (s, 1H), 9.18 (s, 1H), 8.10 (d, *J* = 1.9 Hz, 1H), 8.04 (m, 1H), 7.72 (d, *J* = 8.6 Hz, 2H, Ar-*H*), 7.60 (d, *J* = 8.5 Hz, 2H, Ar-*H*), 7.50 (d, *J* = 8.8 Hz, 1H, Ar-*H*), 7.12 (s, 1H, Ar-*H*), 6.97 (s, 2H), 6.90 (d, *J* = 8.3 Hz, 1H), 6.83 (d, *J* = 1.6 Hz, 1H), 6.04 (s, 2H).^{13}C NMR (101 MHz, DMSO) δ 180.18, 163.15, 161.29, 147.37, 133.74, 133.56, 133.54, 133.27, 126.92, 126.83, 125.54, 125.22, 124.63, 124.46, 120.13, 118.10, 108.28, 106.95, 101.70, 99.98.

4.2. RTK inhibitory activity assay [24]

The *in vitro* RTK inhibition assays of all the title compounds were evaluated using the ADP-Glo™ kinase assay kit (Promega, Madison) with Sorafenib as positive control. The kinase assay was performed in duplicate in a reaction mixture of final volume of 10 μL. General procedures are as the following: Kinases (1.5 ng/μL) were incubated with substrates (1.0 μg/μL), compounds (1.2×10^{-4} - 12 μM) and ATP (250 μM) in a final buffer of Tris 40 mM, $MgCl_2$ 10 mM, BSA 0.1 mg/mL, DTT 1 mM in 384-well plate with the total volume of 5 μL. After the assay plate was incubated at 30 °C for 60 min and cooled for 5 min at room temperature, 5 μL of ADP-Glo™ reagent was added into each well to stop the kinase reaction and deplete the unconsumed ATP. After an additional incubation for 40 min at room temperature, 10 μL of kinase detection reagent was added into the well to convert ADP to ATP. The mixture was incubated for 30 min to produce a luminescence signal. The luminescence was measured using a VICTOR-X multi-label plate reader. The signal was correlated with the amount of ATP present in the reaction and was inversely correlated with the kinase activity.

4.3. Antiproliferative activity against human umbilical vein endothelial cells [25]

The antiproliferative activity of title compounds was evaluated against EA.hy926 cell line by the standard MTT assay *in vitro*. Human umbilical vein endothelial cells (EA.hy926) were purchased from the Cell Bank of Type Culture Collection of Chinese Academy of Science (Shanghai, China). EA.hy926 cells were cultured in DMEM supplemented with 10% (v/v) heat-inactivted fetal calf serum, penicillin (100 U/mL) and streptomycin (100 U/mL). Cultures were maintained at 37 °C in a humidified atmosphere containing 5% CO_2. Briefly, 2×10^4 cells in 100 μL DMEM supplemented with 2% (v/v) heat-inactivated FBS, penicillin (100 U/ml) and streptomycin (100 U/ml) were seeded into 96-well plates. After incubation at 37 °C for 24 h, the test compounds at indicated final concentrations were added to the culture medium and the cells cultures were continued for 48 h. The same volume of double-distilled water was used as the negative control. Then, 22 μL fresh MTT (5 mg/mL) was added to each well and incubated for 4 h at 37 °C. The formazan crystals were dissolved in 100 μL DMSO each well. Supernatant was discarded, and 150 μL DMSO was added to each well. Absorbance values were determined by a microplate reader (Bio-Rad Instruments) at 490 nm. The IC_{50} values were calculated according to inhibition ratios.

4.4. Molecular docking study [26]

Surflex-Dock module of Sybyl-X (Version 2.0, Tripos Inc. St. Louis, MO) was used in molecular docking study. The crystal structures of VEGFR-2 (PDB ID: 4ASD), Tie-2 (PDB ID: 2P4I) [27], and EphB4 (PDB ID: 2X9F) [28] were extracted from the Protein Data Bank. Prior to docking, the ligand was extracted from complex structure and was regarded as the reference molecule. The other ligands and water molecules were removed. All the hydrogen atoms and AMBER7 FF99 charges were added. Compound (**12o**) was depicted and optimized using Powell's method with the Tripos force field with convergence criterion set at 0.05 kcal/(Åmol). Then Gasteiger-Hückel charges were assigned to the small molecule. The residues in a radius 5.0 Å around BAX (the ligand of VEGFR-2 in the crystal complex) were considered as the active site. The optimized conformation of (**12o**) was then docked into the active site of VEGFR-2. Other docking parameters were kept at default.

Acknowledgments

This work was supported by the National Natural Science Foundation of China (*NSFC*, Grant No. 81573285) and the Fundamental Research Funds for the Central Universities (2015qngz13).

Appendix A. Supplementary data

Supplementary data related to this article can be found at http://dx.doi.org/10.1016/j.ejmech.2016.12.059.

References

[1] D. Bouïs, Y. Kusumanto, C. Meijer, N.H. Mulder, G.A. Hospers, A review on pro- and anti-angiogenic factors as targets of clinical intervention, Pharmacol. Res. 53 (2) (2006) 89–103.

[2] X. Zheng, G.Y. Koh, T. Jackson, A continuous model of angiogenesis: initiation, extension, and maturation of new blood vessels modulated by vascular endothelial growth factor, angiopoietins, platelet-derived growth factor-B, and pericytes, Discret. Cont. Dyn-B. 18 (4) (2013) 1109–1154.

[3] S.P. Herbert, D.Y. Stainier, Molecular control of endothelial cell behaviour during blood vessel morphogenesis, Nat. Rev. Mol. Cell Biol. 12 (9) (2011) 551–564.

[4] R.L. Hudkins, N.C. Becknell, A.L. Zulli, T.L. Underiner, T.S. Angeles, L.D. Aimone, M.S. Albom, H. Chang, S.J. Miknyoczki, K. Hunter, S. Jones-Bolin, H. Zhao, E.R. Bacon, J.P. Mallamo, M.A. Ator, B.A. Ruggeri, Synthesis and biological profile of the pan-vascular endothelial growth factor receptor/tyrosine kinase with immunoglobulin and epidermal growth factor-like homology domains 2 (VEGF-R/TIE-2) inhibitor 11-(2-methylpropyl)-12,13-dihydro-2-methyl-8-(pyrimidin-2-ylamino)-4H-indazolo[5,4-a]pyrrolo[3,4-c]carbazol-4-one (CEP-11981): a novel oncology therapeutic agent, J. Med. Chem. 55 (2) (2012) 903–913.

[5] Y. Oike, Y. Ito, K. Hamada, X.Q. Zhang, K. Miyata, F. Arai, T. Inada, K. Araki, N. Nakagata, M. Takeya, Y.Y. Kisanuki, M. Yanagisawa, N.W. Gale, T. Suda, Regulation of vasculogenesis and angiogenesis by EphB/ephrin-B2 signaling between endothelial cells and surrounding mesenchymal cells, Blood 100 (4) (2002) 1326–1333.

[6] Y. Shan, H. Gao, X. Shao, J. Wang, X. Pan, J. Zhang, Discovery of novel VEGFR-2 inhibitors. Part 5: exploration of diverse hinge-binding fragments via core-refining approach, Eur. J. Med. Chem. 103 (2015) 80–90.

[7] P. Su, J. Wang, Y. Shi, X. Pan, R. Shao, J. Zhang, Discovery of biphenyl-aryl ureas as novel VEGFR-2 inhibitors. Part 4: exploration of diverse hinge-binding fragments, Bioorg Med. Chem. 23 (13) (2015) 3228–3236.

[8] W. Lu, P. Li, Y. Shan, P. Su, J. Wang, Y. Shi, J. Zhang, Discovery of biphenyl-based VEGFR-2 inhibitors. Part 3: design, synthesis and 3D-QSAR studies, Bioorg Med. Chem. 23 (5) (2015) 1044–1054.

[9] H. Gao, P. Su, Y. Shi, X. Shen, Y. Zhang, J. Dong, J. Zhang, Discovery of novel VEGFR-2 inhibitors. Part II: biphenyl urea incorporated with salicylaldoxime, Eur. J. Med. Chem. 90 (2015) 232–240.

[10] C. Wang, H. Gao, J. Dong, Y. Zhang, P. Su, Y. Shi, J. Zhang, Biphenyl derivatives incorporating urea unit as novel VEGFR-2 inhibitors: design, synthesis and biological evaluation, Bioorg Med. Chem. 22 (1) (2014) 277–284.

[11] J. Zhang, Y. Zhang, Y. Shan, N. Li, W. Ma, L. He, Synthesis and preliminary biological evaluation of novel taspine derivatives as anticancer agents, Eur. J. Med. Chem. 45 (7) (2010) 2798–2805.

[12] J. Zhang, Y. Zhang, S. Zhang, S. Wang, L. He, Discovery of novel taspine derivatives as antiangiogenic agents, Bioorg Med. Chem. Lett. 20 (2) (2010) 718–721.

[13] B. Dai, J. Qi, R. Liu, J. Zhang, Y. Zhan, Y. Zhang, A novel compound T7 (N-{4'-[(1E)-N-hydroxyethanimidoyl]-3',5,6-trimethoxybiphenyl-3-yl}-N'-[4-(3-morpholin-4-ylpropoxy)phenyl]urea) screened by tissue angiogenesis model and its activity evaluation on anti-angiogenesis, Phytomedicine 21 (12) (2014) 1675–1683.

[14] J. Adams, P. Huang, D. Patrick, A strategy for the design of multiplex inhibitors for kinase-mediated signalling in angiogenesis, Curr. Opin. Chem. Biol. 6 (4) (2002) 486–492.

[15] A.W. Kruger, M.J. Rozema, A. Chu-Kung, J. Gandarilla, A.R. Haight, B.J. Kotecki, S.M. Richter, A.M. Schwartz, Z. Wang, The discovery and development of a safe, practical synthesis of ABT-869, Org, Process Res. Dev. 13 (2009) 1419–1425.

[16] X. Jiang, H. Liu, Z. Song, X. Peng, Y. Ji, Q. Yao, M. Geng, J. Ai, A. Zhang, Discovery and SAR study of c-Met kinase inhibitors bearing an 3-amino-benzo[d]isoxazole or 3-aminoindazole scaffold, Bioorg Med. Chem. 23 (3) (2015) 564–578.

[17] M.M. Vasbinder, B. Aquila, M. Augustin, H. Chen, T. Cheung, D. Cook, L. Drew, B.P. Fauber, S. Glossop, M. Grondine, E. Hennessy, J. Johannes, S. Lee, P. Lyne, M. Mörtl, C. Omer, S. Palakurthi, T. Pontz, J. Read, L. Sha, M. Shen, S. Steinbacher, H. Wang, A. Wu, M. Ye, Discovery and optimization of a novel series of potent mutant B-Raf(V600E) selective kinase inhibitors, J. Med. Chem. 56 (5) (2013) 1996–2015.

[18] J. Yao, J. Chen, Z. He, W. Sun, W. Xu, Design, synthesis and biological activities of thiourea containing sorafenib analogs as antitumor agents, Bioorg Med. Chem. 20 (9) (2012) 2923–2929.

[19] F. Jin, D. Gao, Q. Wu, F. Liu, Y. Chen, C. Tan, Y. Jiang, Exploration of N-(2-aminoethyl)piperidine-4-carboxamide as a potential scaffold for development of VEGFR-2, ERK-2 and Abl-1 multikinase inhibitor, Bioorg Med. Chem. 21 (18) (2013) 5694–5706.

[20] R. Martí-Centelles, E. Falomir, J. Murga, M. Carda, J.A. Marco, Inhibitory effect of cytotoxic stilbenes related to resveratrol on the expression of the VEGF, hTERT and c-Myc genes, Eur. J. Med. Chem. 103 (2015) 488–496.

[21] M. Michailidou, V. Giannouli, V. Kotsikoris, O. Papadodima, G. Kontogianni, I.K. Kostakis, N. Lougiakis, A. Chatziioannou, F.N. Kolisis, P. Marakos, N. Pouli, H. Loutrari, Novel pyrazolopyridine derivatives as potential angiogenesis inhibitors: synthesis, biological evaluation and transcriptome-based mechanistic analysis, Eur. J. Med. Chem. 121 (2016) 143–157.

[22] Y. Zhao, Z. Wang, J. Zhang, H. Zhou, Identification of SENP1 inhibitors through in silico screening and rational drug design, Eur. J. Med. Chem. 122 (2016) 178–184.

[23] Z. Tang, C. Wu, T. Wang, K. Lao, Y. Wang, L. Liu, M. Muyaba, P. Xu, C. He, G. Luo, Z. Qian, S. Niu, L. Wang, Y. Wang, H. Xiao, Q. You, H. Xiang, Design, synthesis and evaluation of 6-aryl-indenoisoquinolone derivatives dual targeting ERα and VEGFR-2 as anti-breast cancer agents, Eur. J. Med. Chem. 118 (2016) 328–339.

[24] J. Kim, S.Y. Kim, S. Kang, H.R. Yoon, B.K. Sun, D. Kang, J.H. Kim, J.J. Song, HSP27 modulates survival signaling networks in cells treated with curcumin and TRAIL, Cell Signal 24 (7) (2012) 1444–1452.

[25] H. Lu, X. Li, J. Zhang, H. Shi, X. Zhu, X. He, Effects of cordycepin on HepG2 and EA.hy926 cells: potential antiproliferative, antimetastatic and anti-angiogenic effects on hepatocellular carcinoma, Oncol. Lett. 7 (5) (2014) 1556–1562.

[26] X. Pan, J. Dong, Y. Shi, R. Shao, F. Wei, J. Wang, J. Zhang, Discovery of novel Bcr-Abl inhibitors with diacylated piperazine as the flexible linker, Org. Biomol. Chem. 13 (25) (2015) 7050–7066.

[27] B.L. Hodous, S.D. Geuns-Meyer, P.E. Hughes, B.K. Albrecht, S. Bellon, J. Bready, S. Caenepeel, V.J. Cee, S.C. Chaffee, A. Coxon, M. Emery, J. Fretland, P. Gallant, Y. Gu, D. Hoffman, R.E. Johnson, R. Kendall, J.L. Kim, A.M. Long, M. Morrison, P.R. Olivieri, V.F. Patel, A. Polverino, P. Rose, P. Tempest, L. Wang, D.A. Whittington, H. Zhao, Evolution of a highly selective and potent 2-(pyridin-2-yl)-1,3,5-triazine Tie-2 kinase inhibitor, J. Med. Chem. 50 (4) (2007) 611–626.

[28] C. Bardelle, B. Barlaam, N. Brooks, T. Coleman, D. Cross, R. Ducray, I. Green, C.L. Brempt, A. Olivier, J. Read, Inhibitors of the tyrosine kinase EphB4. Part 3: identification of non-benzodioxole-based kinase inhibitors, Bioorg Med. Chem. Lett. 20 (21) (2010) 6242–6245.